Inorganic Chemistry
Article

Inorg. Chem. **2010**, *49*, 1471–1480 **1471**
DOI: 10.1021/ic901719t

Two Temperature-Independent *Spinomers* of the Dinuclear Mn(III) Compound $[\{Mn(H_2O)(phen)\}_2(\mu\text{-}2\text{-}ClC_6H_4COO)_2(\mu\text{-}O)](ClO_4)_2$

Verónica Gómez, Montserrat Corbella,* and Gabriel Aullón

Departament de Química Inorgànica, Facultat de Química, Universitat de Barcelona, Martí i Franquès 1-11, 08028 Barcelona, Spain

Received September 1, 2009

Two spin isomers or *spinomers* of $[\{Mn(H_2O)(phen)\}_2(\mu\text{-}2\text{-}ClC_6H_4COO)_2(\mu\text{-}O)](ClO_4)_2$ have been synthesized, characterized, and theoretically analyzed. The thermodynamically most stable, compound **1**, shows a spin ground state $S = 4$, while the kinetically most favorable, compound $\mathbf{2}\cdot H_2O$, shows a spin ground state $S = 0$. Compound **1** exhibits ferromagnetic behavior, with $J = 2.7\ cm^{-1}$, $|D_{Mn}| = 2.06\ cm^{-1}$, $|E_{Mn}| = 0.69\ cm^{-1}$, and $zJ' = -0.11\ cm^{-1}$. Because of the anisotropy of the Mn(III) ions, the ground state $S = 4$ shows zero-field splitting (ZFS) with $|D_4| = 0.51\ cm^{-1}$, appreciably smaller than the D value for the single ion (D_{Mn}), due to the relative orientations of the Jahn−Teller axes of both Mn(III) ions, which are quite perpendicular (102°). Compound $\mathbf{2}\cdot H_2O$ shows antiferromagnetic coupling, with $J = -12.6\ cm^{-1}$ ($H = -JS_1\cdot S_2$ for both compounds). The formation of two *spinomers* has been explained by density functional theory (DFT) studies, which show that the stability of these compounds and their magnetic interaction are very sensitive to the rotation of the phenyl ring with respect to the carboxylate group of the $2\text{-}ClC_6H_4COO$ bridging ligand.

Introduction

Interest in dinuclear Mn(III) complexes with carboxylate ligands is due to their presence in some metalloenzymes, such as Mn-catalase. With the aim of obtaining good model compounds of this enzyme, several dinuclear Mn(III) complexes with a $[Mn_2(\mu\text{-}O)(\mu\text{-}RCOO)_2]^{2+}$ core have been reported in the literature,[1−16] but only some of them are characterized magnetically and by X-ray diffraction.[2−16]

It is well-known that the magnetic interaction for this kind of complex is weak, and may be antiferro- or ferromagnetic,[8] with J values between $+18$ and $-8\ cm^{-1}$. Three possible distortions of the coordination octahedron can be observed because of the Jahn−Teller effect: (a) a compression in the direction of the oxo-bridge, (b) an elongation in the direction of one of the capping ligands, or (c) a rhombic distortion. In general, compounds with an octahedron compressed in the direction of the oxo-bridge show ferromagnetic coupling, while complexes with an elongated octahedron (z axis,

*To whom correspondence should be addressed. E-mail: montse.corbella@qi.ub.es.

(1) (a) Dave, B. C.; Czernuszewickz, R. S. *Inorg. Chim. Acta* **1998**, *281*, 25. (b) Ruiz, R.; Sangregorio, C.; Caneschi, A.; Rossi, P.; Gaspar, A. B.; Real, J. A.; Muñoz, M. C. *Inorg. Chem. Commun.* **2000**, *3*, 361. (c) Reddy, K. R.; Rajasekharan, M. V.; Sukumar, S. *Polyhedron* **1996**, *15*, 4161. (d) Albela, B.; Corbella, M.; Ribas, J. *Polyhedron* **1996**, *15*, 91. (e) Tanase, T.; Lippard, S. J. *Inorg. Chem.* **1995**, *34*, 4682. (f) Bossek, U.; Wieghardt, K.; Nuber, K.; Weiss, J. *Inorg. Chim. Acta* **1989**, *165*, 123. (g) Mandal, S. K.; Armstrong, W. H. *Inorg. Chim. Acta* **1995**, *229*, 261. (h) Reddy, K. R.; Rajasekharan, M. V.; Sukumar, S. *Polyhedron* **1996**, *15*, 4161. (i) Blackman, A. G.; Huffman, J. C.; Lobkovsky, E. B.; Christou, G. *J. Chem. Soc., Chem. Commun.* **1991**, 989. (j) Mok, H. J.; Davis, J. A.; Pal, S.; Mandal, S. K.; Armstrong, W. H. *Inorg. Chim. Acta* **1997**, *263*, 385.

(2) (a) Mahapatra, S.; Lal, T. K.; Mukherjee, R. *Inorg. Chem.* **1994**, *33*, 1579. (b) Lal, T. K.; Mukherjee, R. *Inorg. Chem.* **1998**, *37*, 2373.

(3) Wieghardt, K.; Bossek, U.; Ventur, D.; Weiss, J. *J. Chem. Soc., Chem. Commun.* **1985**, 347.

(4) Wieghardt, K.; Bossek, U.; Nuber, B.; Weiss, J.; Bonvoisin, J.; Corbella, M.; Vitols, S. E.; Girerd, J. J. *J. Am. Chem. Soc.* **1988**, *110*, 7398.

(5) Bolm, C.; Meyer, N.; Raabe, G.; Weyhermüller, T.; Bothe, E. *Chem. Commun.* **2000**, 2435.

(6) Sheats, J. E.; Czernuszewicz, R. S.; Dismukes, G. C.; Rheingold, A. L.; Petrouleas, V.; Stubbe, J. A.; Armstrong, W. H.; Beer, R. H.; Lippard, S. J. *J. Am. Chem. Soc.* **1987**, *109*, 1435.

(7) Wu, F. J.; Kurtz, D. D., Jr.; Hagen, K. S.; Nyman, P. D.; Debrunner, P. G.; Vankai, V. A. *Inorg. Chem.* **1990**, *29*, 5174.

(8) Hotzelmann, R.; Wieghardt, K.; Flörke, U.; Haupt, H. J.; Weatherburn, D. C.; Bonvoisin, J.; Blondin, G.; Girerd, J. J. *J. Am. Chem. Soc.* **1992**, *114*, 1681.

(9) Ménage, S.; Girerd, J. J.; Gleizes, A. *J. Chem. Soc., Chem. Commun.* **1988**, 431.

(10) Vincent, J. B.; Folting, K.; Huffman, C. J.; Christou, G. *Biochem. Soc. Trans.* **1988**, 822.

(11) Vincent, J. B.; Tsai, H. L.; Blackman, A. G.; Wang, S.; Boyd, P. D.; Folting, K.; Huffman, J. C.; Lobkovsky, E. B.; Hendrickson, D. N.; Christou, G. *J. Am. Chem. Soc.* **1993**, *115*, 12353.

(12) Corbella, M.; Costa, R.; Ribas, J.; Fries, P. H.; Latour, J. M.; Ohrstrom, L.; Solans, X.; Rodríguez, V. *Inorg. Chem.* **1996**, *35*, 1857.

(13) Chen, C.; Zhu, H.; Huang, D.; Wen, T.; Liu, Q.; Liao, D.; Cui, J. *Inorg. Chim. Acta* **2001**, *320*, 159.

(14) Fernández, G.; Corbella, M.; Alfonso, M.; Stoeckli-Evans, H.; Castro, I. *Inorg. Chem.* **2004**, *43*, 6684.

(15) Mitra, K.; Mishra, D.; Biswas, S.; Lucas, C. R.; Adhikary, B. *Polyhedron* **2006**, *25*, 1681.

(16) Fernández, G.; Corbella, M.; Aullón, G.; Maestro, M. A.; Mahía, J. *Eur. J. Inorg. Chem.* **2007**, 1285.

Published on Web 01/19/2010

Scheme 1. Schematic Structure of the Dinuclear Mn(III) Complexes, with the Distortion Axes of the Octahedron

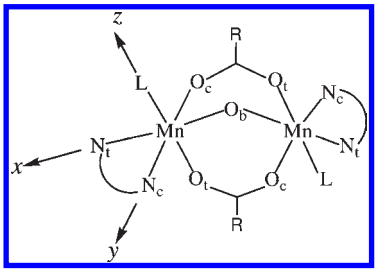

Scheme 1) show antiferromagnetic coupling. When the distortion is rhombic, the magnetic interaction can be either ferro- or antiferromagnetic.[8,12,16]

Tridentate amines favor a compressed octahedron and, in most cases, a significant ferromagnetic interaction was found.[2−5,8] However, some tridentate amines lead to a rhombic distortion, and in these cases, the complexes show a weak antiferromagnetic interaction.[6,7]

When the capping ligand is bpy (2,2′-bipyridine), the sixth position of the octahedron is occupied by a monodentate ligand; this situation provides greater flexibility of the coordination octahedron and different types and degrees of distortion can be found.[12,16] However, there is only one compound which displays a compressed octahedron around the Mn(III) ions, $[\{Mn(bpy)(N_3)\}_2(\mu\text{-}O)(\mu\text{-}C_6H_5COO)_2]$, and it shows an important ferromagnetic coupling.[10,11] For the rest of the compounds, the octahedral distortion can be elongated, in the direction of the monodentate ligand, or rhombic. As was reported in previous works, the degree of this distortion and the magnetic properties are very sensitive to the monodentate ligand and its donor or acceptor character.[11,16] Moreover, for these compounds, the magnetic behavior also depends on the carboxylate ligand. A comparative study of $[\{Mn(bpy)(L)\}_2(\mu\text{-}O)(\mu\text{-}2\text{-}RC_6H_4COO)_2]^{n+}$ compounds with R = Me or F, L = H_2O, NO_3 or ClO_4, and n = 2, 1, or 0, show that the antiferromagnetic interaction is more important for a donor R (Me) and a π-acid ligand L (NO_3).[16]

As a continuation of the magneto-structural correlations for $[\{Mn(L)(nn)\}_2(\mu\text{-}O)(\mu\text{-}RCOO)_2]X_2$ compounds, we report two new compounds with the same formula $[\{Mn(H_2O)(phen)\}_2(\mu\text{-}2\text{-}ClC_6H_4COO)_2(\mu\text{-}O)](ClO_4)_2$ but with different magnetic behavior (ferro- or antiferromagnetic interaction). Both compounds show the same composition and atomic connectivity and the same stereochemistry. However, they differ in their magnetic behavior and consequently, in their spin ground state (S = 4 and S = 0). Therefore, these compounds are spin isomers or *spinomers*. This term is used for spin-crossover complexes, where the spin state changes with the temperature.[17] In contrast, and for the first time, the two *spinomers* reported here are temperature-independent. With the aim of finding an explanation for the formation of these two *spinomers*, an analysis of the structural data has been carried out with DFT calculations.

Experimental Section

Synthesis. All manipulations were carried out at room temperature under aerobic conditions. Reagents and solvents were obtained from commercial sources and used without further purification. NBu_4MnO_4 was prepared as described in the literature.[18] Yields were calculated from stoichiometric reaction. ***Caution!*** *Perchlorate salts of compounds containing organic ligands are potentially explosive. Only small quantities of these compounds should be prepared and handled behind suitable protective shields.*

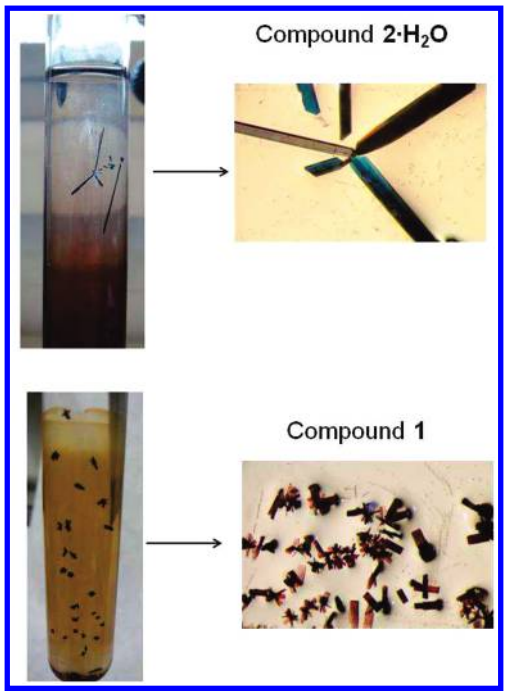

Figure 1. Photographs of $[\{Mn(H_2O)(phen)\}_2(\mu\text{-}2\text{-}ClC_6H_4COO)_2(\mu\text{-}O)](ClO_4)_2$ crystals.

$[\{Mn(H_2O)(phen)\}_2(\mu\text{-}2\text{-}ClC_6H_4COO)_2(\mu\text{-}O)](ClO_4)_2$ (1) and ($2\cdot H_2O$). Both compounds were synthesized as follows: 2-ClC_6H_4COOH (0.25 g, 1.60 mmol) in MeCN (∼7 mL) was added to a solution of $Mn(ClO_4)_2\cdot 6H_2O$ (0.46 g, 1.28 mmol) in MeCN (∼5 mL). Then, NBu_4MnO_4 (0.11 g, 0.32 mmol) dissolved in MeCN (∼10 mL) was added to the above-mentioned solution, which immediately turned dark brown. Finally, an MeCN solution of 1,10-phenanthroline (phen) (0.32 g, 1.60 mmol) was added, and the resulting solution (total volume 30 mL) was stirred for 15 min. Slow evaporation of the mother liquor in the refrigerator led to the precipitation of a microcrystalline black solid (**1**). However, concentration of the initial solution under reduced pressure until ∼5 mL led to the precipitation of a dark brown solid (**2**). Both products were dried in air. Compound **1**: yield 0.33 g (40%). Anal. Calcd for $C_{38}H_{28}Cl_4Mn_2N_4O_{15}$ (1032.33 g mol^{-1}): C, 44.21; H, 2.73; N, 5.43; Cl, 13.74. Found: C, 44.1; H, 2.6; N, 5.5; Cl, 13.7. IR (KBr, cm^{-1}): 1598 (s), 1587 (s), 1564 (m), 1519 (m), 1426 (m), 1392 (vs), 1340 (m), 1110 (s), 1086 (vs), 874 (m), 860 (m), 846 (m), 760 (m), 749 (m), 738 (m), 721 (s), 652 (m), 624 (m). Molar conductivity in MeCN, 10^{-3} M: 314 Ω^{-1} cm^3 mol^{-1}. Compound **2**: yield 0.30 g (36%). Anal. Calcd for $C_{38}H_{28}Cl_4Mn_2N_4O_{15}$ (1032.33 g mol^{-1}): C, 44.21; H, 2.73; N, 5.43; Cl, 13.74. Found: C, 44.0; H, 2.8; N, 5.5; Cl, 13.8. IR (KBr, cm^{-1}): 1598 (s), 1587 (s), 1563 (m), 1519 (m), 1427 (s), 1385 (s), 1341 (m), 1120 (vs), 1089 (s), 1052 (s), 875 (m), 851 (m), 756 (m), 739 (m), 721 (s), 654 (m), 624 (m). Molar conductivity in MeCN, 10^{-3} M: 326 Ω^{-1} cm^3 mol^{-1}. Crystals suitable for X-ray diffraction of **1** and $\mathbf{2}\cdot H_2O$ were obtained as follows: the mother liquor was diluted with more MeCN in a 1:1 ratio, then CH_2Cl_2 (1:1) was added, and finally, this mixture was layered with hexanes. After 1 month some elongated green crystals of compound $\mathbf{2}\cdot H_2O$ were formed in the hexanes layer.

(17) Cirera, J.; Ruiz, E.; Alvarez, S. *Inorg. Chem.* **2008**, *47*, 2871.

(18) Sala, T.; Sargenti, M. V. *J. Chem. Soc., Chem. Commun.* **1978**, 253.

Table 1. X-ray Crystallographic Data for Compounds **1** and **2**·H_2O

	1	**2**·H_2O
chemical formula	$C_{38}H_{28}Cl_4Mn_2N_4O_{15}$	$C_{38}H_{30}Cl_4Mn_2N_4O_{16}$
formula weight /g mol^{-1}	1032.32	1050.32
T/K	100(2)	100(2)
λ (Mo Kα)/Å	0.71073	0.71073
crystal system	*Pbca*	$P2_1/n$
space group	orthorhombic	monoclinic
crystal size/mm	0.33 × 0.17 × 0.02	0.51 × 0.16 × 0.05
a/Å	17.6317(8)	10.5737(3)
b/Å	20.8001(8)	22.7311(7)
c/Å	22.7553(10)	17.0612(5)
α/deg	90	90
β/deg	90	95.9790(10)
γ/deg	90	90
V/Å^3	8345.3(6)	4078.4(2)
Z	8	4
ρ_{calcd}/g cm^{-3}	1.643	1.706
μ/mm^{-1}	0.937	0.962
F(000)	4176	2116
Θ range/deg.	1.76 to 26.40	1.50 to 26.35
limiting indices	h = 0→22, k = 0→25, l = 0→28	h = −13→13, k = 0→28, l = 0→21
data/restraints/parameters	8538/0/641	8297/21/604
goodness-of-fit on F^2	0.991	1.136
final R indices [$I > 2\sigma(I)$]	R1[a] = 0.0497	R1[a] = 0.0758
	wR2[b] = 0.1071	wR2[b] = 0.1623
R indices (all data)	R1[a] = 0.1015	R1[a] = 0.0971
	wR2[b] = 0.1243	wR2[b] = 0.1697

[a] $R1 = \sum||F_o| - |F_c||/\sum|F_o|$. [b] $wR2 = \{\sum w(F_o^2 - F_c^2)^2/\sum w(F_o^2)^2\}^{1/2}$.

Later, new crystals with different shape and color were formed in the MeCN−CH_2Cl_2 layer, corresponding to compound **1** (Figure 1).

Physical Measurements. Analyses of C, H, N and Cl were carried out by the "Servei de Microanàlisi" of the "Consell Superior d'Investigacions Científiques (CSIC)". Infrared spectra were recorded on KBr pellets, in the range 4000−400 cm^{-1}, with a Termo Nicolet Avatar 330 FT-IR spectrometer. Conductivity measurements were carried out with a HACH HQ40d instrument, at room temperature. UV−visible spectra were performed in a CARY 100 Scan Spectrophotometer, at room temperature. Magnetic susceptibility measurements between 2−300 K and magnetization measurements, at 2 K, between 0−5 T, and in the 1.8−6.8 K and 0.5−5 T range, were carried out in a SQUID magnetometer Quantum Design Magnetometer, model MPMP at the "Unitat de Mesures Magnètiques (Universitat de Barcelona)". Two different magnetic fields were used for the susceptibility measurements, 300 G (2−5 K) and 3000 G (2−300 K), with superimposable graphs. Pascal's constants were used to estimate the diamagnetic corrections for the compounds. The fit was performed by minimizing the function $R = \sum[(\chi_M T)_{exp} - (\chi_M T)_{calc}]^2/\sum(\chi_M T)_{exp}]^2$.

X-ray Diffraction Data Collection and Refinement. X-ray crystallographic data for crystals of **1** and **2**·H_2O were collected at 100 K. All measurements were made on a Bruker Apex-2 diffractometer with graphite monochromated Mo Kα radiation (λ = 0.7107 Å). The structures were solved using the SIR97 program[19] and refined using the SHELXL97 program.[20] Hydrogen atoms were treated by a mixture of independent and constrained refinement. Crystal data collection and refinement parameters are given in Table 1.

Computational Details. Unrestricted density functional calculations were carried out using the Gaussian03 package,[21] with the B3LYP hybrid method.[22] An all-electron triple-ζ basis set was used for all atoms.[23] The evaluation of the spin states gap was carried out by non-projected DFT calculations using the methodology described elsewhere, in which broken-symmetry formalism for an antiferromagnetically coupled state is applied,[24] and these calculations provide quantitative results in comparison with very accurate theoretical methods.[25]

Structural Analysis. Experimental structural data were retrieved from the Cambridge Structural Database (Version 5.30 with one update, November 2008).[26] A search for structures with a monosubstituted 2-halobenzoate ligand acting as a bridge between two transition metal ions was carried out, finding a total of 16 (8 refcodes), 23 (8), 4 (2), and 5 (3) independent fragments for F, Cl, Br, and I derivatives, respectively.

Results and Discussion

Synthesis. The dinuclear Mn(III) compound [{Mn((H_2O)(phen)}$_2$(μ-2-ClC_6H_4COO)$_2$(μ-O)](ClO_4)$_2$ was

(19) Altomare, A.; Burla, M. C.; Camalli, M.; Cascarano, G. L.; Giacovazzo, C.; Guagliardi, A.; Moliterni, A. G. G.; Polidori, G.; Spagna, R. *SIR97: A new tool for crystal structure determination and refinement; J. Appl. Crystallogr.* **1999**, *32*, 115.

(20) Sheldrick, G. M. *SHELXL97, A Program for Crystal Structure Refinement*; University of Göttingen: Göttingen, Germany, 1997.

(21) Frisch, M. J.; Trucks, G. W.; Schlegel, H. B.; Scuseria, G. E.; Robb, M. A.; Cheeseman, J. R.; Montgomery, J. A., Jr.; Vreven, T.; Kudin, K. N.; Burant, J. C.; Millam, J. M.; Iyengar, S. S.; Tomasi, J.; Barone, V.; Mennucci, B.; Cossi, M.; Scalmani, G.; Rega, N.; Petersson, G. A.; Nakatsuji, H.; Hada, M.; Ehara, M.; Toyota, K.; Fukuda, R.; Hasegawa, J.; Ishida, M.; Nakajima, T.; Honda, Y.; Kitao, O.; Nakai, H.; Klene, M.; Li, X.; Knox, J. E.; Hratchian, H. P.; Cross, J. B.; Adamo, C.; Jaramillo, J.; Gomperts, R.; Stratmann, R. E.; Yazyev, O.; Austin, A. J.; Cammi, R.; Pomelli, C.; Ochterski, J. W.; Ayala, P. Y.; Morokuma, K.; Voth, G. A.; Salvador, P.; Dannenberg, J. J.; Zakrzewski, V. G.; Dapprich, S.; Daniels, A. D.; Strain, M. C.; Farkas, O.; Malick, D. K.; Rabuck, A. D.; Raghavachari, K.; Foresman, J. B.; Ortiz, J. V.; Cui, Q.; Baboul, A. G.; Clifford, S.; Cioslowski, J.; Stefanov, B. B.; Liu, G.; Liashenko, A.; Piskorz, P.; Komaromi, I.; Martin, R. L.; Fox, D. J.; Keith, T.; Al-Laham, M. A.; Peng, C. Y.; Nanayakkara, A.; Challacombe, M.; Gill, P. M. W.; Johnson, B.; Chen, W.; Wong, M. W.; Gonzalez, C.; Pople, J. A. *Gaussian 03*, Revision C.2; Gaussian Inc.: Wallingford, CT, 2004.

(22) (a) Becke, A. D. *J. Chem. Phys.* **1993**, *98*, 5648. (b) Lee, C.; Yang, W.; Parr, R. G. *Phys. Rev. B* **1988**, *37*, 785.

(23) Schaefer, A.; Horn, H.; Ahlrichs, R. *J. Chem. Phys.* **1992**, *97*, 2571.

(24) Ruiz, E.; Cano, J.; Alvarez, S.; Alemany, P. *J. Comput. Chem.* **1999**, *20*, 1391.

(25) Ruiz, E.; Alvarez, S.; Cano, J.; Polo, V. *J. Chem. Phys.* **2005**, *123*, 164110.

(26) Allen, F. H. *Acta Crystallogr., Sect. A* **2002**, *58*, 380.

obtained by a comproportionation reaction between $Mn(ClO_4)_2$ and Bu_4NMnO_4, in the presence of 2-ClC_6H_4COOH and 1,10-phenanthroline (phen). This compound crystallizes in two different forms, compounds **1** and **2**·H_2O, which show different stability and solubility. When the mother liquor is sufficiently concentrated, the first product to appear is compound **2**·H_2O, more favorable kinetically than compound **1**. However, slower crystallization yields the thermodynamically more stable compound **1**. This is also observed when the mother solution mixed with CH_2Cl_2 is layered under hexanes. Compound **2**·H_2O crystallizes first as elongated green prisms in the hexanes layer, and later, compound **1** crystallizes in the MeCN−CH_2Cl_2 layer, as brown-green aggregates (Figure 1).

Compounds **1** and **2**·H_2O can be differentiated by their IR spectra. In the regions around ∼850 cm^{-1} and ∼740 cm^{-1}, compound **1** shows one band more than compound **2**·H_2O: in the region of ∼850 cm^{-1} compounds **1** and **2**·H_2O show three and two bands, respectively, and in the region of ∼740 cm^{-1}, four and three bands, respectively. These dissimilarities may be due to the small structural differences in the $[Mn_2(\mu\text{-RCOO})_2(\mu\text{-O})]^{2+}$ core. Moreover, these compounds show two strong bands at ∼1600 and ∼1390 cm^{-1} arising from the asymmetric and symmetric vibrations from the carboxylate groups of the 2-chlorobenzoate ligand. The values of $\Delta = \nu_a(COO) - \nu_s(COO)$, being about 200 cm^{-1}, fall in the range of reported values for carboxylate groups coordinated in a bridging mode.[27] Broad bands at ∼1100 cm^{-1} and a band of moderate intensity at 624 cm^{-1} are assigned to the perchlorate ions. The Mn−O−Mn group usually displays a band at ∼730 cm^{-1}, which is masked by phen bands. This ligand shows characteristic bands at 1519, 1427, ∼875, ∼855, and 721 cm^{-1}.

Molar conductivity values of these compounds in MeCN solution are close to the expected values for 1:2 electrolytes in said solvent.[28] Thus the dinuclear structure of these compounds is retained in solution. The electronic spectra of these compounds in MeCN at 25 °C show three bands of high intensity at 202, 225, and 271 nm which correspond to intra ligand transitions, a broad band at ∼700 nm which could be assigned to d−d transitions and two shoulders at ∼500 and 520 nm. The band at ∼700 nm is very sensitive to the presence of water or humidity, which causes the signal to disappear. The spectra of both compounds are very similar, and no noticeable change was observed with time.

Description of Structures. $[\{Mn(H_2O)(phen)\}_2(\mu\text{-2-}ClC_6H_4COO)_2(\mu\text{-O})](ClO_4)_2$ (1) and $[\{Mn(H_2O)(phen)\}_2(\mu\text{-2-}ClC_6H_4COO)_2(\mu\text{-O})](ClO_4)_2\cdot H_2O$ (2·H_2O). The cationic complex $[\{Mn(H_2O)(phen)\}_2(\mu\text{-2-}ClC_6H_4COO)_2(\mu\text{-O})]^{2+}$ of both compounds is displayed in Figures 2 and 3. Selected bond lengths and angles are listed in Table 2.

The Mn(III) ions are bridged through two 2-chlorobenzoate and one oxo ligands. The octahedral coordination of each manganese ion is completed by a phen ligand and one water molecule. The structural parameters of compounds **1** and **2**·H_2O agree with those reported for

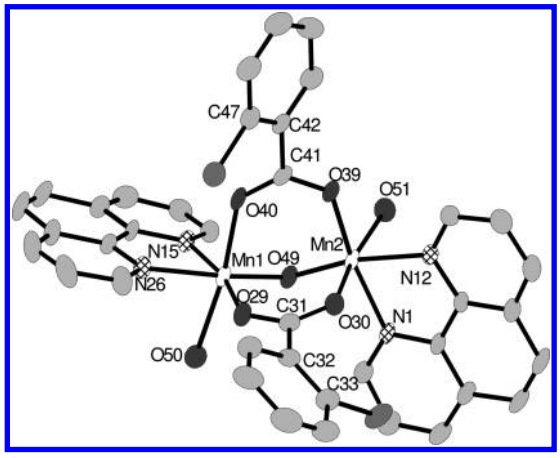

Figure 2. Crystal structure of the cationic complex $[\{Mn(H_2O)(phen)\}_2(\mu\text{-2-}ClC_6H_4COO)_2(\mu\text{-O})]^{2+}$ for **1**, showing the atom labeling scheme and ellipsoids at 50% probability. Hydrogen atoms have been omitted for clarity.

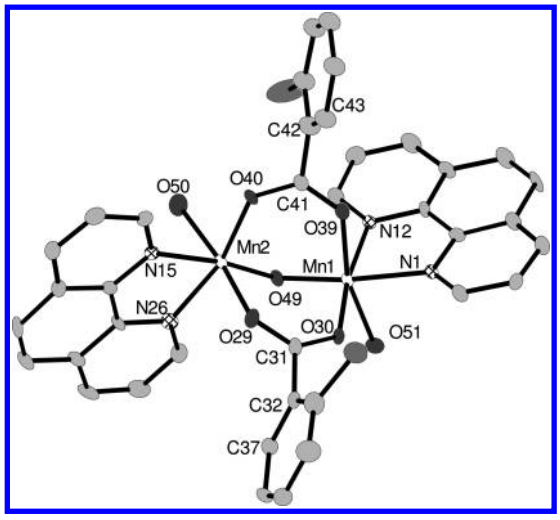

Figure 3. Crystal structure of the cationic complex $[\{Mn(H_2O)(phen)\}_2(\mu\text{-2-}ClC_6H_4COO)_2(\mu\text{-O})]^{2+}$ for **2**·H_2O, showing the atom labeling scheme and ellipsoids at 50% probability. Hydrogen atoms have been omitted for clarity.

analogous compounds with the same $[Mn_2(\mu\text{-O})(\mu\text{-RCOO})_2]^{2+}$ core.[2−16] The Mn···Mn distance is ∼3.14 Å, and the Mn−O−Mn angle is 122.9° for both compounds. The $Mn-O_{bridge}$ bond lengths are ∼1.79 Å, the Mn−N bond lengths are ∼2.08 Å, and the $Mn-O_w$ bond lengths are ∼2.21 Å. The carboxylate bridging ligands are coordinated in a *syn-syn* mode, with one of the oxygen atoms placed *trans* to the water molecule, with a Mn−O distance of ∼2.17 Å, and the other oxygen atom *trans* to a nitrogen atom of the phen, with a shorter Mn−O distance (∼1.97 Å).

Considering the x axis in the oxo-bridge direction and the z axis in the monodentate ligand direction (O_w) (Scheme 1), approximate values of the octahedron axes lengths can be found by addition of Mn−ligand distances: $d(Mn-O_b) + d(Mn-N_t) = x$ (x axis), $d(Mn-O_c) + d(Mn-N_c) = y$ (y axis) and $d(Mn-O_t) + d(Mn-O_w) = z$ (z axis). The distortion parameter (dp), calculated as $(z - y)/(y - x)$,[16] is indicative of the kind of distortion of the octahedron: high values correspond to an elongation in the direction of the monodentate ligand, while low

(27) Deacon, B.; Phillips, R. J. *Coord. Chem. Rev.* **1980**, *33*, 227.
(28) Geary, W. J. *Coord. Chem. Rev.* **1971**, *7*, 81.
(29) Kahn, O. *Molecular Magnetism*: Wiley-VCH: New York, 1993.

Table 2. Selected Bond Lengths (Å) and Angles (deg) for Compounds **1** and **2**·H_2O

1		**2**·H_2O	
Mn(1)−O(49)	1.788(2)	Mn(1)−O(49)	1.790(4)
Mn(1)−O(29)	1.977(3)	Mn(1)−O(30)	1.968(4)
Mn(1)−N(26)	2.080(3)	Mn(1)−N(1)	2.081(4)
Mn(1)−N(15)	2.083(3)	Mn(1)−N(12)	2.073(4)
Mn(1)−O(40)	2.150(3)	Mn(1)−O(39)	2.180(4)
Mn(1)−O(50)	2.187(3)	Mn(1)−O(51)	2.216(4)
Mn(1)−Mn(2)	3.1387(7)	Mn(1)−Mn(2)	3.1470(11)
Mn(2)−O(49)	1.785(2)	Mn(2)−O(49)	1.793(4)
Mn(2)−O(39)	1.968(2)	Mn(2)−O(40)	1.956(4)
Mn(2)−N(12)	2.081(3)	Mn(2)−N(15)	2.066(4)
Mn(2)−N(1)	2.083(3)	Mn(2)−N(26)	2.080(4)
Mn(2)−O(30)	2.149(3)	Mn(2)−O(29)	2.172(4)
Mn(2)−O(51)	2.203(3)	Mn(2)−O(50)	2.217(4)
H(50B)···O(67)	1.911(66)	H(50A)···O(70w)	2.123(42)
H(50A)···O(64)	2.197(70)	H(50A)···O(68)	2.553(50)
H(50A)···O(61A)	2.377(68)	H(50B)···O(61)	2.075(46)
H(51B)···O(66A)	1.975(69)	H(51A)···O(65)	2.045(70)
H(51A)···O(62A)	2.057(47)	H(51B)···O(62)	2.021(73)
		O(70A)···O(63)	2.946(10)
Mn(1)−O(49)−Mn(2)	122.90(14)	Mn(1)−O(49)−Mn(2)	122.9(2)
O(49)−Mn(1)−N(26)	169.72(12)	O(49)−Mn(1)−N(1)	170.60(17)
O(29)−Mn(1)−N(15)	167.96(12)	O(30)−Mn(1)−N(12)	171.50(16)
O(40)−Mn(1)−O(50)	169.48(12)	O(39)−Mn(1)−O(51)	166.03(15)
O(49)−Mn(2)−N(12)	169.77(11)	O(49)−Mn(2)−N(15)	172.70(17)
O(39)−Mn(2)−N(1)	168.84(11)	O(40)−Mn(2)−N(26)	165.02(17)
O(30)−Mn(2)−O(51)	168.83(11)	O(29)−Mn(2)−O(50)	171.90(15)
O(50)−Mn(1)−Mn(2)−O(51)	102.11(14)	O(51)−Mn(1)−Mn(2)−O(50)	88.26(18)
O(30)−C(31)−C(32)−C(33)	44.44(54)	O(29)−C(31)−C(32)−C(37)	81.84(66)
O(40)−C(41)−C(42)−C(47)	47.61(51)	O(39)−C(41)−C(42)−C(43)	73.99(76)
Mn(1)−O(40)−O(39)−Mn(2)	0.76(14)	Mn(1)−O(39)−O(40)−Mn(2)	11.84(20)
Mn(1)−O(29)−O(30)−Mn(2)	1.70(15)	Mn(1)−O(30)−O(29)−Mn(2)	11.41(21)

values correspond to a rhombic distortion of the octahedron. Both compounds show $z > y > x$, the z axis being the Jahn−Teller distortion direction. Nevertheless, compound **1** shows a shorter z distance than compound **2**·H_2O, leading to a greater rhombic character. The distortion parameters for **1** and **2**·H_2O are 1.53 and 2.04, respectively.

The relative disposition of the manganese coordination octahedra is almost perpendicular in both compounds, with O_w−Mn−Mn−O_w torsion angles of 102.11° for compound **1** and 88.26° for compound **2**·H_2O. The carboxylate group and the phenyl ring are not coplanar, with torsion angles of 44.44 and 47.61° for compound **1**, and 81.84 and 73.99° for compound **2**·H_2O. The twist of the aromatic ring could be due to the steric hindrance between phen ligands and the chloro-substituent, in *ortho* position.

In compound **1**, the Cl atoms of the two carboxylate bridges are found on opposite sides of the aromatic ring, while in compound **2**·H_2O one of the Cl atoms is disordered over both *ortho* positions.

In compound **1**, the dinuclear complexes are connected through perchlorate anions, which are bonded to the water ligand via hydrogen bonds, generating a one-dimensional (1D) system (Figure 4). In compound **2**·H_2O the hydrogen bonding network is more complex because of the presence of a crystallization water molecule. As in compound **1**, the perchlorate anions bridge two dinuclear complexes through hydrogen bonds with the water ligand, and moreover, the perchlorate anions are hydrogen-bonded to the crystallization water molecule generating a chain (Supporting Information, Figure S1). Hydrogen bond distances for both compounds are collected in Table 2.

Magnetic Properties. Magnetic susceptibility data were recorded for compounds **1** and **2**·H_2O from room temperature to 2 K. $\chi_M T$ versus T plots of both compounds are shown in Figure 5. At 300 K, the $\chi_M T$ values are 6.16 $cm^3\ mol^{-1}$ K for compound **1** and 5.46 $cm^3\ mol^{-1}$ K for compound **2**·H_2O, close to the expected value for two uncoupled high-spin Mn(III) ions (6.0 $cm^3\ mol^{-1}$ K). For compound **1**, $\chi_M T$ values increases as the temperature falls, reaching a maximum value of 7.32 $cm^3\ mol^{-1}$ K at 13 K; below this temperature, $\chi_M T$ values fall until 6.10 $cm^3\ mol^{-1}$ K at 2 K. This behavior is characteristic of ferromagnetic coupling. The $\chi_M T$ expected value for a system with a ground state $S = 4$ is 10 $cm^3\ mol^{-1}$ K; the lower value found at 13 K and the decreasing of $\chi_M T$ below this temperature could be explained by the presence of zero-field splitting (ZFS) in the ground state and/or intermolecular antiferromagnetic interactions. In contrast, for compound **2**·H_2O, $\chi_M T$ values decrease when the temperature descends; this behavior is characteristic of an antiferromagnetic coupling between the two Mn(III) ions. For this compound, the χ_M versus T plot shows a maximum of 0.052 $cm^3\ mol^{-1}$ at 35 K, in agreement with an antiferromagnetic interaction and an $S = 0$ ground state (Figure 5, inset). It is interesting to note that the $\chi_M T$ versus T plots for **2** (microcrystalline sample) and **2**·H_2O (crushed crystals) are superimposable.

The spin Hamiltonian $H = -JS_1 \cdot S_2$ was used to fit the experimental data, assuming that the two Mn(III) ions present the same g value. For compound **2**·H_2O, the best fit of χ_M T data was obtained with $J = -12.6\ cm^{-1}$ and $g = 2.02$, with $R = 7.4 \times 10^{-5}$; similar values were obtained by fitting the χ_M data ($J = -12.0\ cm^{-1}$ and $g = 2.01$, with $R = 8.5 \times 10^{-4}$).

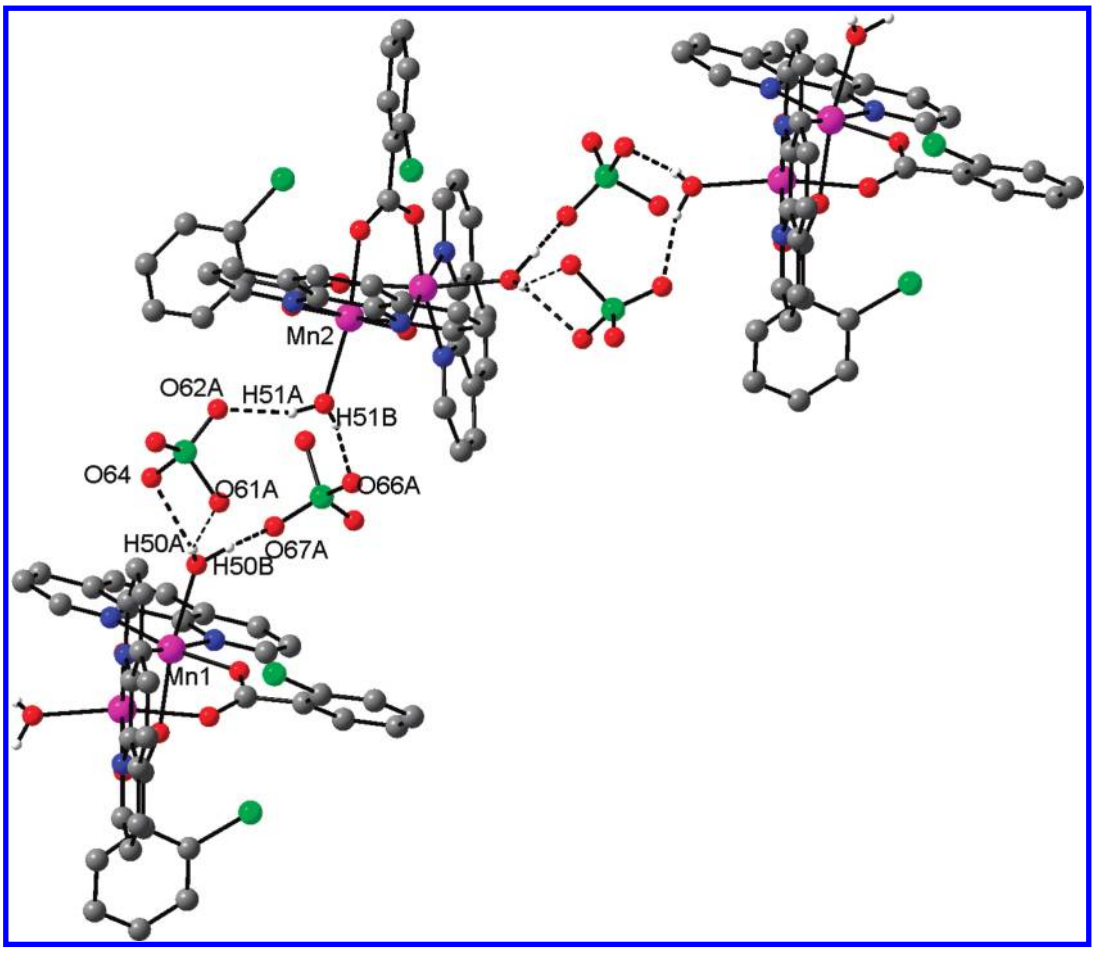

Figure 4. Diagram of the hydrogen bonds present in the crystal structure of **1**, between perchlorate anions and water ligands of the dinuclear complex, generating a one-dimensional system.

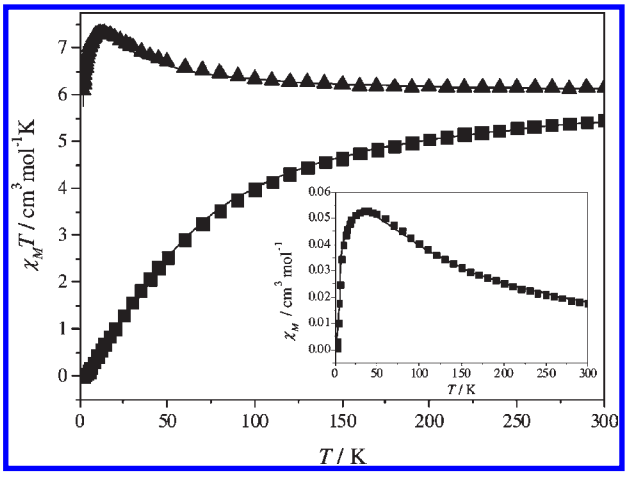

Figure 5. $\chi_M T$ vs T and χ_M vs T (inset) plots for compounds **1** (▲) and **2**·H_2O (■). The solid line is the best fit to the experimental data.

For the ferromagnetic compound (**1**), with the aim of fitting the whole curve, the Mn(III) dinuclear complex equation was modified by including the intermolecular interactions (zJ')[29] or the axial ZFS parameter (D) in the ground state $S = 4$, where the Hamiltonian describing the ZFS was $H_D = D\,[S_z^2 - S(S+1)/3]$. The best reproduction of the magnetic behavior was obtained when intermolecular interactions were considered, the best fit parameters being $J = +1.4$ cm^{-1} and $zJ' = -0.35$ cm^{-1}. This agrees with the existence of hydrogen bonds between the dinuclear complexes and the counter-anions. On the other hand, important differences in the shape of the graph at low temperatures were obtained when the axial ZFS in the ground state was considered. Taking into account the rhombic distortion of the octahedron around the Mn(III) ions, the ion ZFS parameters, D_{Mn} and E_{Mn}, should be considered. Thus, with the aim of including these parameters and the intermolecular interactions in the calculation, the final fit of the experimental $\chi_M T$ data was carried out with the Magpack-fit program,[30] with $|E_{Mn}| = |D_{Mn}|/3$. Attempts to fit the experimental data without intermolecular interactions (zJ') were unsuccessful. The best fit was obtained with $J = +2.7$ cm^{-1}, $|D_{Mn}| = 2.06$ cm^{-1}, $|E_{Mn}| = 0.69$ cm^{-1}, $zJ' = -0.11$ cm^{-1}, and $g = 2.0$, with $R = 1.98 \times 10^{-4}$ (J values using the $H = -JS_1 \cdot S_2$ convention). The D_{Mn} value for the Mn(III) ion in this compound is of the same order as the values collected by R. Boca for high-spin Mn(III) mononuclear complexes.[31] Magnetization measurements at 2 K and 50000 G show a $M/N\mu_B$ value of 5.96, in agreement with the weak ferromagnetic interaction.

(30) *Magpack* program: Borrás-Almenar, J. J.; Clemente-Juan, J. M.; Coronado, E.; Tsukerblat, B. *J. Comput. Chem.* **2003**, *9*, 985. Fit: DSTEPIT program. Program 66, Quantum Chemistry Program Exchange, Indiana University, Bloomington, IN.

(31) Boca, R. *Coord. Chem. Rev.* **2004**, *248*, 757.

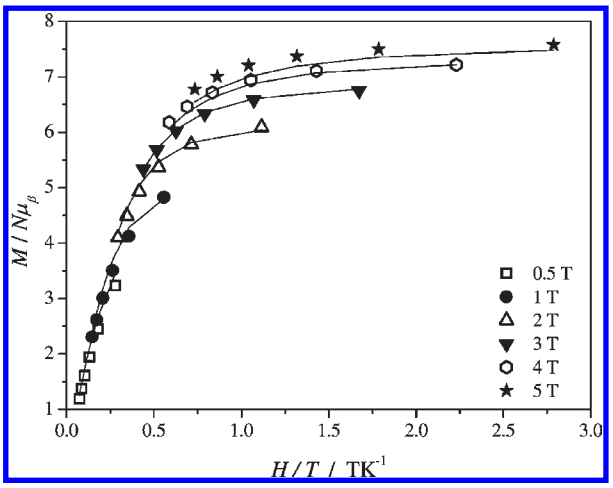

Figure 6. $M/N\mu_B$ vs H/T plots for compound **1** at different magnetic fields: 0.5, 1, 2, 3, 4, and 5 T. The solid line is the best fit to the experimental data.

To check the presence of magnetic anisotropy, magnetization versus temperature measurements were carried out at six different fields (0.5−5 T) in the 1.8−6.8 K range. $M/N\mu_B$ versus H/T plots are shown in Figure 6.

The non-superposition of the various isofield lines indicates significant ZFS within the ground state. The experimental data were fitted by full diagonalization of the energy matrices based on the ZFS Hamiltonian H_D for an isolated ground state $S = 4$.[32] The best fit was obtained with $|D_4| = 0.51$ cm^{-1} and $g = 1.98$, with $R = 5.24 \times 10^{-4}$. It is interesting to note that despite the significant D_{Mn} value, because of the Jahn−Teller distortion, the quite perpendicular disposition of the elongation axes leads to a small value of the ZFS parameter for the ground state D_4.

Alternating current susceptibility experiments were performed to determine whether compound **1** exhibited slow magnetization relaxation. It was studied in the 1.7−50 K temperature range with a 3 G alternating current (ac) field oscillating at 1000 Hz. The out-of-phase ac susceptibility signal (χ_M'') was zero, indicating a fast magnetization relaxation rate, therefore compound **1** does not behave as a SMM despite showing ZFS and a ground state $S = 4$.

The magnetic coupling constants found for compounds **1** and **2**·H_2O are in the range of those reported for analogous Mn(III) dinuclear complexes. Table 3 collects the compounds with benzoate derivative bridging ligands. As has been indicated, for this kind of compound the magnetic interaction is very sensitive to the distortion of the coordination octahedra and the kind of monodentate ligand (σ or π-acid ligand).[16] For the seven compounds reported previously in the literature, the magnetic properties are influenced by both factors. As can be seen in Table 3, these compounds differ in the monodentate ligand and/or in the X group of the carboxylate ligand. On the other hand, compounds **1** and **2**·H_2O show exactly the same cationic complex $[\{Mn(phen)_2(H_2O)_2\}_2(\mu\text{-}2\text{-}ClC_6H_4CO_2)_2(\mu\text{-}O)]^{2+}$ and, in spite of this, they show different spin ground states, $S = 4$ for **1** and $S = 0$ for **2**·H_2O, so these complexes could be considered as magnetic *spinomers*.

Table 3. Magnetic Coupling Constants[a] for $[\{Mn(nn)(L)\}_2(\mu\text{-}XC_6H_4COO)_2(\mu\text{-}O)]^{m+}$ Complexes, Where the Monodentate Ligand (L) Could Be Neutral (H_2O) or Anionic

compound	X	nn	L	J/cm^{-1}	ref
2·H_2O	2-Cl	phen	H_2O	−12.6	this work
A	2-Me	bpy	H_2O/ClO_4	−5.6	16
B	2-F	bpy	H_2O/ClO_4	−3.5	16
C	2-Me	bpy	H_2O/NO_3	−0.5	16
D	2-F	bpy	H_2O/NO_3	1.4	16
E	H	bpy	OH/NO_3	2.0	12
1	2-Cl	bpy	H_2O	2.7	this work
F	2-COO	bpy	H_2O/NO_3	4.7	13
G	H	phen	N_3	17.6	11

[a] $H = -J S_1 \cdot S_2$. **A** $[\{Mn(bpy)(H_2O)\}_2(\mu\text{-}2\text{-}MePhCOO)_2(\mu\text{-}O)][\{Mn(ClO_4)(bpy)\}_2(\mu\text{-}2\text{-}MePhCOO)_2(\mu\text{-}O)](ClO_4)_2 \cdot 0.5CH_2Cl_2$; **B** $[\{Mn(bpy)(H_2O)\}(\mu\text{-}2\text{-}FPhCOO)_2(\mu\text{-}O\{Mn(ClO_4)(bpy)\}]ClO_4 \cdot 2CH_2Cl_2$; **C** $[\{Mn(bpy)(H_2O)\}(\mu\text{-}2\text{-}MePhCOO)_2(\mu\text{-}O\{Mn(NO_3)(bpy)\}]NO_3 \cdot 1.5CH_3CN \cdot 2H_2O$; **D** $[\{Mn(bpy)(H_2O)\}(\mu\text{-}2\text{-}FPhCOO)_2(\mu\text{-}O\{Mn(NO_3)(bpy)\}]NO_3 \cdot H_2O$; **E** $[\{Mn(OH)(bpy)\}(\mu\text{-}PhCOO)_2(\mu\text{-}O\{Mn(NO_3)(bpy)\}]$; **F** $[\{Mn(bpy)(H_2O)\}_2(\mu\text{-}2\text{-}COOC_6H_4COO)_2(\mu\text{-}O)][\{Mn(bpy)(H_2O)\}(\mu\text{-}2\text{-}COOC_6H_4COO)_2(\mu\text{-}O)\{Mn(bpy)\ (NO_3)\}](NO_3)_3$; **G** $[\{Mn(N_3)(bpy)\}_2(\mu\text{-}PhCOO)_2(\mu\text{-}O)]$.

It is necessary to emphasize that the importance of these *spinomers* is due to the fact that they show exactly the same ligands, therefore the electronic effects of the ligands depend only on the structural parameters. The cationic complexes of **1** and **2**·H_2O show different degrees of distortion: compound **2**·H_2O shows an elongated octahedral environment around the Mn(III) ions (distortion parameter, dp = 2.04) while compound **1** displays a rhombic distortion (dp = 1.53). As was indicated, compounds with elongated octahedra usually show a greater antiferromagnetic interaction, whereas the rhombic distortion could give ferro- or antiferromagnetic interactions. So, the results obtained for both *spinomers* are in the expected range. Nevertheless, it is difficult to justify the 15 cm^{-1} difference between the magnetic coupling constants (J) taking into consideration only the distortion of the octahedron around the Mn(III) ions. It is well-known that small structural changes affect the magnetic properties of this kind of dinuclear complex. So, a more detailed analysis of the structure and the electronic effect produced by these changes is necessary to understand the behavior of $[\{Mn(H_2O)_2(phen)_2\}_2(\mu\text{-}2\text{-}ClC_6H_4CO_2)_2(\mu\text{-}O)](ClO_4)_2$ compound.

This compound could be obtained as two isomers, one of them favored kinetically and with a spin ground state $S = 0$ (*spinomer* **2**) and the other one thermodynamically most stable with a spin ground state $S = 4$ (*spinomer* **1**). Both isomers show similar hydrogen bonds between the ClO_4^- anions and the water ligand of the dinuclear complex, but despite the similarity of their structures, there are two structural parameters well differentiated: the elongation or rhombicity of the octahedron, discussed previously, and the orientation of the phenyl ring of the carboxylate bridge.

Theoretical Analysis. Complex $[\{Mn(H_2O)_2(phen)_2\}_2(\mu\text{-}2\text{-}ClC_6H_4CO_2)_2(\mu\text{-}O)]^{2+}$ is of special interest because of the variation of the spin ground state of both isomeric forms. This difference in the electronic structure has been associated with changes in some geometric parameters described above, and it is widely known in mononuclear

(32) Software package supplied by E. Rivière, Université Paris Sud (Orsay), France.

complexes.[17] However, a theoretical analysis for this dinuclear complex is needed to understand its electronic structure.

From the experimental structural data of both *spinomers*, theoretical calculations were carried out to find the ground state and the magnetic coupling constant, in each case. The calculated J values found for compounds **1** and **2**·H_2O are −7.8 and −21.5 cm^{-1}, respectively. Therefore, from these calculations, both *spinomers* should have a singlet as ground state, resulting from an antiferromagnetic coupling between the Mn(III) ions. These results are noticeably different from the experimental ones (+2.7 and −12.6 cm^{-1}); however, the difference between the experimental and calculated J value for each *spinomer* is less than 10 cm^{-1}. It is necessary to mention that this deviation is of the order of discrepancy for density function calculation,[25] as theoretical results are acutely sensitive to the computational details,[33] such as the basis set or the functional method. In spite of this, the calculated and experimental results agree in the fact that *spinomer* **2** shows a larger antiferromagnetic coupling than **1** and, moreover, the difference between the J values for both *spinomers* is similar (calculated, 13.7 vs experimental, 15.3 cm^{-1}). Figure 7 shows a comparative scheme of the experimental and calculated energy spin levels. Since several methodologies have been developed to estimate J values from ferromagnetic and antiferromagnetic states, accurate energies are found for the former, whereas less rigorous values are obtained for the latter. By comparing these results, it can be concluded that the computational study has overestimated the stability of $S = 0$ state by ∼10 cm^{-1} (0.1 kJ mol^{-1}).

As the magnetic behavior has been determined by structural data, the analysis of the geometric parameters of both isomers was considered. A detailed study shows an important change in the rotation between the carboxylate group and the phenyl ring, defined as ω (Scheme 2), having experimental values of ∼46 and ∼78° for compounds **1** and **2**·H_2O respectively.

With the aim of analyzing the influence of the rotation angle (ω) on the relative stability of the molecular geometry, a new calculation was carried out with the experimental structural data of *spinomer* **1** modifying only the ω angle from 0 to 360°. Although this is a rough approximation, it can be helpful to understand the structural preferences of this compound. Figure 8 shows the profile of the relative energy for this complex versus the rotation angle ω. This plot presents two minima at ∼70 and ∼290°, which correspond to an alternated configuration of the 2-chlorobenzoate bridge, where the phenyl group is practically perpendicular to the O−C−O plane. Although the most stable configuration corresponds to the minimum at ∼290°, the difference in energy between both minima is less than 4 kcal mol^{-1}. Furthermore, this plot shows two maxima at ∼30° and ∼170°, with energy values about 50 and 27 kcal mol^{-1} above the minimum, respectively, in which ligand···ligand interactions are determining to the relative stability. As an example of these interactions, repulsions between the halogen atoms and the carboxylate group (in eclipsed conformation, i.e., at 0° and 180°) or π-system of 1,10-phenanthroline are found. These high energies would suggest that the conversion between both minima can be rejected.

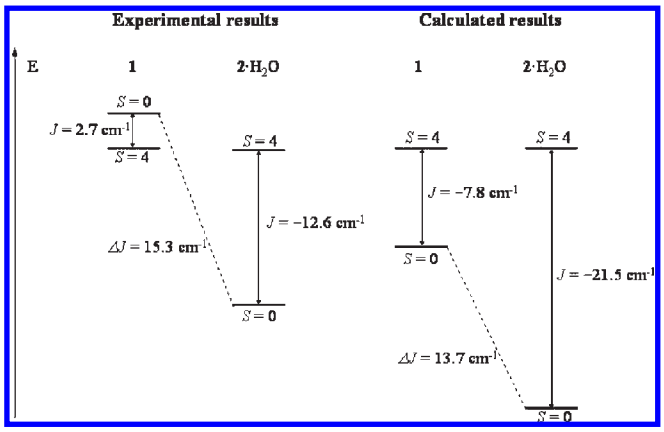

Figure 7. Schematic drawing showing the experimental and calculated relative energy of the spin states $S = 0$ and $S = 4$, for the two *spinomers* **1** and **2**·H_2O.

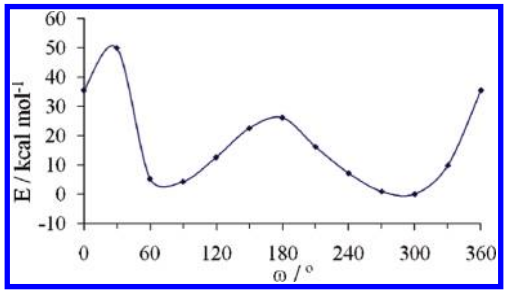

Figure 8. Calculated relative energy for complex [{Mn(H_2O)(phen)}$_2$-(μ-2-ClC_6H_4COO)$_2$(μ-O)]$^{2+}$ as a function of ω, keeping all the other geometric parameters as experimental structure of **1**.

Scheme 2. Rotation Angle (ω) of the Phenyl Ring in Relation to the Mn−O−C−O−Mn Plane

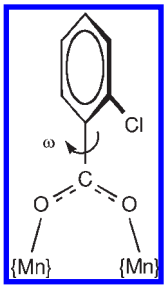

From the experimental data, the formation of the complex with a fully alternated conformation (compound **2**·H_2O, $\omega \sim 78°$) should point to a higher kinetic stability (the first to crystallize), whereas the staggered complex (compound **1**, $\omega \sim 46°$) should be the thermodynamically most stable product. In agreement with the thermodynamic preference of the staggered conformation, when left to stand for a long time in solution, compound **2**·H_2O forms compound **1**. The more stable staggered conformation of benzoate ligand in the complex is due to the presence of weak ligand···ligand interactions and probably different crystal-packing requirements. Consequently, with the aim of understanding the experimental results, new calculations with the full

(33) Ruiz, E.; Rodríguez-Fortea, A.; Tercero, J.; Cauchy, T.; Massobrio, C. *J. Chem. Phys.* **2005**, *123*, 074102.

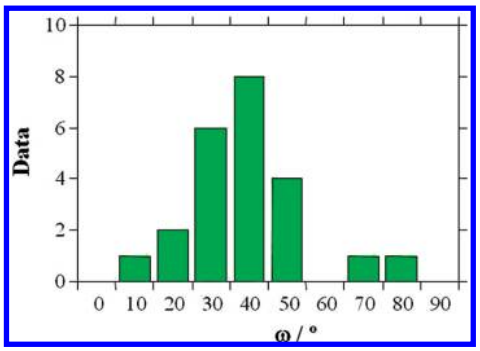

Figure 9. Histogram of experimental angle ω retrieved from Cambridge Structural Database for 2-chlorobenzoate bridging ligands between two transition metals.

optimization of complex **1** were carried out, obtaining a molecular geometry with staggered conformation ω = 37°, close to the experimental value of 46°.

To confirm the relative stabilities of the different conformations of 2-chlorobenzoate ligand, experimental structures where this ligand bridges two transition metals ions were searched in the Cambridge Structural Database. The distribution of the rotation angle ω, shown in Figure 9 for the 2-ClC_6H_4COO ligand, agrees with the theoretical result reported here: with this ligand the majority of compounds show a rotation angle between 30 and 40°. Similar results were obtained from all 2-halobenzoate ligands (Supporting Information, Figure S3), in which the size of halogen is likely to be decisive in adjusting the molecular structure: for compounds with 2-fluorobenzoate ligand the most usual rotation angle is between 10−20°, while compounds with bromo- and iodo-derivatives show ω angles between 40−50°.

At this point it only remains to rationalize the different magnetic behavior of both *spinomers*. For dinuclear Mn(III) compounds with 4 electrons in each manganese ion (i and j), the magnetic coupling constant is $J = (1/16)\sum J_{ij}$.[29] Because of the presence of one empty d orbital in each manganese ion, there are 8 crossing interactions between each single occupied d orbital and the empty (x^2-y^2) orbital; this kind of interaction is postulated as ferromagnetic.[29] The most important antiferromagnetic contribution to the magnetic behavior is due to the π^* interaction through the oxo-bridging ligand, $xz(1)/xy(2)$ (local axis as Scheme 1). Other antiferromagnetic contributions could be the π^* interaction $xy(1)/xz(2)$ and $z^2(1)/z^2(2)$, sensitive to the Mn−O_b−Mn angle, and the $z^2(1)/xz(2)$ and $xy(1)/z^2(2)$ interactions. Subsequently, there is an important number of interactions of both signs, ferro- and antiferromagnetic, and the resultant magnetic behavior of these compounds is due to a complicated balance of these contributions. Taking into account that the Mn−O_b−Mn angle is the same in both compounds, this manner of interaction could be expected to be very similar. However, there are three interaction pathways where the carboxylate bridge could contribute via a π^* overlap: the $xz(1)/xy(2)$ and $xy(1)/xz(2)$ orbitals of the Mn(III) ions could interact with one of the carboxylate ligands, perpendicular or in the same Mn−O_b−Mn plane, respectively; and the $yz(1)/yz(2)$ orbitals of the Mn(III) ions with both carboxylate ligands. It is interesting to remark that this interaction is only due to the carboxylate bridges. Therefore the contribution of the carboxylate to the magnetic interaction could be very sensitive to the structural changes in this ligand.

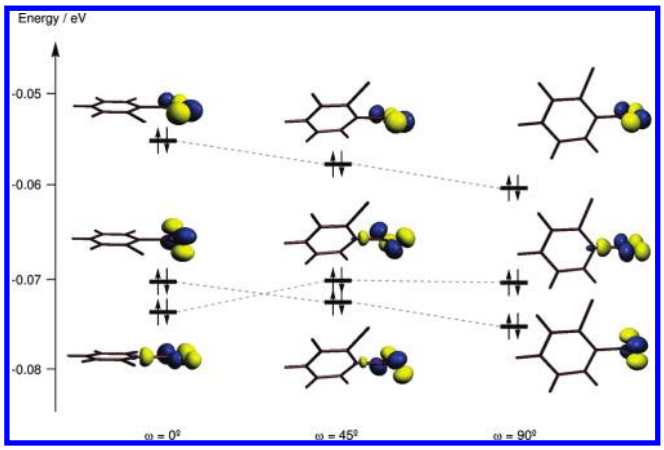

Figure 10. Energy diagram for the three highest occupied orbitals of the 2-chlorobenzoate anion as a function of the rotation angle ω. Contour shown corresponds to 0.1 electrons.

With the aim of analyzing if the rotation angle of the phenyl ring could affect the magnetic properties the molecular orbital topology of this anion was investigated. Figure 10 shows the energy diagram with the topology of the three highest occupied molecular orbitals of this ligand, at three different rotation angles (0°, 45°, and 90°). The highest and lowest in energy are σ lone-pairs, antisymmetric and symmetric combinations, respectively. The other orbital is a π lone-pair, and its topology is very sensitive to the rotation angle: at 0 and 90° it shows a similar topology, with a good disposition for π overlap with the d orbitals of the manganese ion, while at 45° the energy of this orbital decreases and most important, the topology changes and decreases the π-interaction, reducing the antiferromagnetic contribution. The topology and energy of the symmetric combination of the σ lone-pairs is also sensitive to the rotation angle, with a different topology at 45°. This orbital, at 90°, could be sensitive also to the planarity of the Mn−O−C−O−Mn group. Small deviations of the planarity, like in *spinomer* **2**, lead to a new way for a π interaction.

So, the rotation of the phenyl ring affects the topology of the lone-pairs of the oxygen atoms of the carboxylate, and could be crucial to the balance between the ferro- and the antiferormagnetic contributions, with the result of two compounds with different spin ground state: **1** with $\omega \sim 46°$ and $S = 4$ and **2**·H_2O with $\omega \sim 78°$ and $S = 0$. It is expected that this trend could be qualitatively observed in other families of compounds, but depending on its importance, the effects would be more significant on the magnetic coupling constant.

Finally, a more detailed study of electronic density from natural population analysis was made. Both compounds show identical spin density for $S = 0$ and $S = 4$ (± 3.71 and $+ 3.78$ in each manganese atom respectively). Moreover, variations of less than 0.01 electrons are found in both cases when the ω angle is modified.

Conclusions

Well-differentiated crystals of two *spinomers* of [{Mn(H_2O)$_2$(phen)$_2$}$_2$(μ-2-$ClC_6H_4CO_2$)$_2$(μ-O)](ClO_4)$_2$ have been

obtained. The most favorable kinetically ($2\cdot H_2O$) shows an alternated conformation of the carboxylate bridge (phenyl ring ~ perpendicular to the OCO plane) and presents an antiferromagnetic coupling between both Mn(III) ions, so a spin ground state $S = 0$. The most stable thermodynamically (**1**) shows weak interactions such as ligand···ligand contacts that lead to a staggered conformation of the carboxylate bridge (phenyl ring at ~45° to the OCO plane), and displays a ferromagnetic behavior, with a spin ground state $S = 4$. The analysis of structural data for complexes with $2\text{-}XC_6H_4COO$ ligands, bridging two transition metal ions, shows that the rotation angle between the phenyl ring and the OCO plane is sensitive to the volume of the X group. For the Cl derivatives, the most frequent angle is ~30−40°, like the angle found for *spinomer* **1**.

DFT calculations with the crystallographic data of **1** and $2\cdot H_2O$ confirm the different magnetic behavior, with a difference on the magnetic coupling constant of ~14 cm^{-1}. Moreover, these calculations show a greater stability of the staggered conformation of the benzoate derivative ligand, in comparison with the alternated conformation. The different conformation of these ligands affects the topology of the lone-pair combinations of the oxygen atoms, and this fact could be decisive in the net balance between the ferro- and antiferromagnetic contributions to the magnetic behavior.

After these results, it would be interesting to obtain analogous compounds with different substituents in two isomeric forms, with the aim of having more proof of the effect of the twist of the phenyl ring on the magnetic behavior.

Acknowledgment. The authors thank the Ministerio de Educación y Ciencia (CTQ2009-07264/BQU and CTQ2008-06670-C02-01/BQU) and the Comissió Interdepartamental de Recerca i Innovació Tecnològica de la Generalitat de Catalunya (CIRIT) (2009-SGR1454 and 2005/SGR-00036) for financial support. V.G. thanks the Ministerio de Ciencia e Innovación for the Ph.D. grant BES-2007-15668.

Supporting Information Available: X-ray crystallographic data in Cif format for complexes **1** and $2\cdot H_2O$. View of the hydrogen bonds present in the crystal structure of $2\cdot H_2O$, between the perchlorate anions and the water ligands of the dinuclear complex, and with the crystallization water molecule (Figure S1). Histogram for experimental angle ω retrieved from Cambridge Structural Database for 2-halobenzoate bridging ligands between two transition metals (Figure S2). Atomic coordinates for full optimized geometry of cation $[\{Mn(H_2O)(phen)\}_2(\mu\text{-}2\text{-}ClC_6H_4COO)_2(\mu\text{-}O)]^{2+}$ with ground state $S = 4$ (Table S1). This material is available free of charge via the Internet at http://pubs.acs.org.